Optical properties of CdTe/ZnTe core/shell quantum dots suitable for targeted bioimaging

R. KOSTIĆ, D. STOJANOVIĆ*
University of Belgrade, Institute of Physics, Center for Solid State Physics and New Materials, P. O. Box 68, 11080 Belgrade, Serbia

In this work we present results of our calculations of CdTe/ZnTe core/shell quantum dots (QDs) of very small size capable for targeted bioimaging. The transition energy of the electron and hole system confined in a CdTe/ZnTe core/shell sphere is obtained by the effective-mass approximation. Optical properties are analyzed as function of QD size and spatial composition and compared to already known experimental results. CdTe/ZnTe core/shell-structured QDs are perspective to use in biomedical applications because: they exhibit strong luminescence and low toxicity (compared to the CdTe QD); shell of wide-gap semiconductor protects core from degradation; they have long-term colloidal and optical stability; their surface can be passivated with biocompatible functional molecules; they can be produced in small size, less than 5 nm. These properties enable their use for targeted bioimiging.

(Received December 1, 2011; accepted February 20, 2012)

Keywords: Quantum dots, Optical properties of nanocrystals and nanoparticles, Quantum efficiency

1. Introduction

Owing to their high photo-stability, good luminescence efficiency, high oscillator strength and large emission tunability II-VI core/shell semiconductor quantum dots (QD) serve as useful fluorescent labels. Surface is found to plays a vital role on their electronic and optical properties, because quantum dots have very high surface to volume ratio [1]. Organic ligands are used to passivate the nanocrystaline surface, but effective passivation of anionic, as well as cationic surface sites, is not accomplished by these organic cappants. Inorganic semiconductor shell on quantum dots (core) can passivate both cationic and anionic dangling bonds and provide good electronic chemical surface passivation. The shell can have different functions in core/shell quantum dots, depending on the energy gap and the relative position of the energy levels of the involved semiconductors. In type-I core/shell quantum dots shell of higher energy gap material is coating the narrower energy gap core material. Type-I nanoheterostructures typically provide an order of magnitude higher photoluminescence (PL) quantum efficiency. This increase in PL quantum efficiency is a sign of proper passivation of surface dangling bonds and nonradiative recombination sites, as well as improved confinement of electrons and holes in the quantum dot core. Change of charge carrier wave functions leads to enhanced luminescence quantum efficiency.

Since hydrophilic QDs were first used as fluorescence probes in cellular labeling [2, 3] QDs have attracted widespread attention from the field of biology and medicine [4] and achieved great progress in biomedical applications [5, 7]. When they are used in biomedical research, water solubility is required for QDs. In contrast to organic fluorescent probes, QDs have much better photostability, which is the most attractive characteristic for cellular labeling, especially in long-term imaging such as tracking the transportation processes in cells and probing the path of labeled molecules [8, 9].

CdTe QDs, with tunable optical properties that cover from visible to the near-infrared spectral region, have found numerous applications ranging from electronics to sensors. The use of CdTe QDs for biological applications is still limited because they are more toxic than the core/shell CdSe/ZnS, CdSe/CdS/ZnS or InP/ZnS QDs. Core/shell QDs are more suitable for use in biomedical applications because they exhibit strong luminescence with low toxicity. CdS and ZnS wide gap semiconductors are commonly used to coat QDs. Wide band gap ZnS coating (E_g= 3.5 eV) should provide the best shell coverage for the CdTe core (E_g= 1.5 eV) but the large lattice mismatch between CdTe and ZnS lattice parameters (≈ 20%) induces strain at the interface. In the case of CdTe/ZnTe core/shell QDs, very small lattice mismatch (≈ 6%) leads to a uniform epitaxial growth of the ZnTe shell around the CdTe core. Result is a low defects density in the shell and high quantum yield (QY) values.

Recently a new method for synthesizing robust luminescent CdTe/ZnTe QDs with high photoluminescent efficiency and stability have been developed [10]. The CdTe/ZnTe QDs were synthesized in a one-pot method and capped with amino acid cystine, which contains both carboxyl and amine functional groups on their surfaces for bioconjugation. In this technique, the as-synthesized QDs were monodisperse, ultrasmall (diameter less than 5 nm), biocompatible and nontoxic. These QDs fulfill all the conditions for in vitro and in vivo targeted bioimaging. Photoluminescent measurements of synthesized CdTe/ZnTe QDs have been presented [10].

In this paper we present a study of the evolution of (CdTe)ZnTe QDs electronic structure. Our calculations were performed in the well known and widely used effective mass approximation (EMA) [11-13]. We analyzed experimental results presented in [10].

2. Models and results

We assume that the dot consists of a spherical CdTe core (radius r_0=r_c) surrounded by a ZnTe concentric shell (from r_0 to r_1) without alloying at the surface. Electrons and holes in such a system are characterized by their effective masses and potentials. Parameters for the calculation, effective masses of carriers and conduction and valence band offsets between materials, are transferred from literature [14,15].

For core/shell structure presented in Fig. 1. there are three regions of different effective masses:

$$m^*_{e,h}(r)=\begin{cases} m^*_{e,h_0} & r \le r_0 = r_C \\ m^*_{e,h_1} & r_0 < r \le r_1, \\ m^*_{e,h_2} & r > r_1 \end{cases}$$

In this case m^*_{e,h_0} are effective masses of CdTe ($m^*_{e_0} = m^*_{e_{CdTe}} = 0.0999\, m_e$, $m^*_{h_0} = m^*_{h_{CdTe}} = -0.51\, m_e$) and m^*_{e,h_1} are effective masses of ZnTe ($m^*_{e_1} = m^*_{e_{ZnTe}} = 0.116\, m_e$, $m^*_{h_1} = m^*_{h_{ZnTee}} = -0.6\, m_e$), Table I. We assigned a potential energy of zero inside CdTe core V_0 and barrier height of 670 meV for the electron and 100 meV for the hole to tunnel into the ZnS shell, Table I. The boundary conditions on the outside of the shell can be chosen as infinite potential well or third material. Infinite potential barriers artificially increase confinement energies. Using a third material as a finite barrier is more realistic. We assumed that the electron must tunnel through a 4 eV and hole through a 10 eV potential barrier to extend into the surrounding organic matrix. We chose to use free-electron masses in the outside material, very large energy gap and dielectric constant close to water value. Qualitative trends in the results are not sensitive to these values.

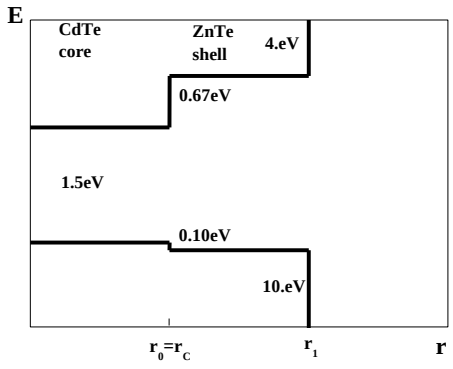

Fig. 1. Energetic scheme of (CdTe)ZnTe core/shell nanoheterostructure.

Considering that electron and hole spectra are mainly formed by size quantization, the stationary Schrödinger equation for a single particle may be expressed as:

$$\left(-\frac{\hbar^2}{2m^*}\nabla^2 + V(r)\right)\Psi(\vec{r}) = E\Psi(\vec{r})$$

For spherically symmetric potential $V(r)$ the separation of radial and angular coordinates leads to:

$$\Psi_{nlm}(\vec{r}) = R_{nl}(r)Y_{lm}(\theta,\varphi)\,.$$

$R_{nl}(r)$ is the radial wave function, and $Y_{lm}(\theta,\varphi)$ is a spherical harmonic. n is the solution number for one l, and l and m are the angular momentum quantum numbers.

For a spherical potential with stepwise constant value V_0=0 in CdTe core, V_1 in ZnTe layer and V_2 in surrounding material the radial function $R_{nl,q}(r)$, consist of three parts, because it speeds through three different regions:

$$R_{nl}=\begin{cases} R^0_{nl} = A^l_0 j_l(K_0 r) & r \le r_C = r_0 \\ R^1_{nl} = A^l_1 j_l(K_1 r) + B^l_1 n_l(K_1 r) & r_0 \le r \le r_1 \\ R^2_{nl} = A^l_2 h^{(1)}_l(K_2 r) & r \ge r_1 \end{cases}$$

$K_i = \sqrt{\frac{2m^*_i}{\hbar^2}(E - V_i)}$ $\quad i = 0,1,2$; j_l, n_l, $h^{(1)}_l$ are Bessel, Neumann and Hankel spherical functions. Solutions already satisfy conditions to be regular when r = 0 and to vanish sufficiently rapidly when $r \to \infty$. The solution must satisfy boundary conditions:

$$\begin{aligned} R^i_{nl}(r)\big|_{r=r_i} &= R^{i+1}_{nl,}(r)\big|_{r=r_i} && i = 0,1 \\ \frac{1}{m^*_i}\frac{dR^i_{nl}(r)}{dr}\Big|_{r=r_i} &= \frac{1}{m^*_{i+1}}\frac{dR^{i+1}_{nl}(r)}{dr}\Big|_{r=r_i} && i = 0,1 \end{aligned} \qquad (1)$$

Equations (1) lead to a system of four linear equations for the four unknown coefficients. It has nontrivial solutions only if its determinant

$$D_l = D_l(E_{nl}) = 0. \qquad (2)$$

Once the eigenvalues E_{nl} are determined from (2), the linear equations can be solved yielding the coefficients to be a function of one of them. The last undetermined coefficient is determined by the normalization condition. As all solutions are determined, we can unify them to get the complete picture of eigensolutions E_{nl} and corresponding wave functions R_{nl}. These calculations were performed independently for electrons and holes (procedure is similar), giving the confinement energies E^e_{nl} and E^h_{nl}, and wave functions R^e_{nl} and R^h_{nl}. Once the electron and hole wave functions are known, radial probability in the system give an illustrative picture of electron and hole spatial localization.

We focused our analysis to l = 0, n=1 state of zero angular momentum, so called S-symmetry. Wave function of state l = 0, m = 0 is dependent only on r. Principal quantum number n is numeration of the solution, n = 1,2,3.

From the electron and hole wave functions, the Coulomb interaction of electron and hole can be calculated. Energy of Coulomb interaction is given by:

$$E_C = -e^2 \int\int \frac{\left|R^e(r_e)\right|^2 \left|R^h(r_h)\right|^2}{\varepsilon(r_e, r_h)\left|r_e - r_h\right|} r_e^{\,2} r_h^{\,2} dr_e dr_h$$

$\varepsilon(r_e,r_h)$ is the high energy dielectric permittivity.

The transition electronic energy (E_{10}) is sum of the CdTe gap energy, corresponding electron and hole eigenvalues and the Coulomb energy

$$E_{10} = E_G + E_{10}^e + E_{10}^h + E_C \ . \qquad (3)$$

To get insight into the (CdTe)ZnTe QD optical properties we calculated E_{10} energies for CdTe core radius from 1 nm to 2.5 nm and ZnTe shell thickness from 0.3 to 2.1 nm. Results of our calculations are presented in Fig. 2. We calculated energies for bare CdTe dots too (points in Fig. 2. on position ZnTe shell thickness equal zero). We present results for few core radii to illustrate behavior. These dimensions give the final dot dimension of about 3-5 nm, as QDs produced in [10]. The transition electronic energies are in interval 1.8 - 2.5 eV i.e. PL peak positions are in interval 496 - 688 nm. These wavelengths are marked in Fig. 2. (right). We also calculated electron and hole wave functions, radial probability functions and wave function overlaps for each configuration. Radial probabilities for four selected structures are presented in Figs. 3. and 4.

Table 1. Material parameters of the system: a - lattice constant, E_g- energy gap, V_e, V_h- conduction and valence offsets, m^*-effective masses, m_e-electron mass, ε- dielectric constants.

	a(Å)	E_g(eV)	V_e(eV)	V_h(eV)	m_e^*/m_e	m_h^*/m_e	ε
CdTe	6.478	1.5			0.0999	0.51	7.1
ZnTe	6.103	2.27	0.67	0.1	0.116	0.6	6.7

In bare CdTe QD electron and hole are confined in a deep potential well, 4 eV barrier for the electron and 10 eV barrier for hole to tunnel to surrounding medium. The electron wave function spreads over the entire dot and partially tunnels into the surrounding medium, with discontinuity in the slope due to the abrupt change in effective mass and potential. In case of small radius (r_c= 1.25 nm in Fig. 3.a) maximum of electron radial probability is close to the surface. Radius probability for big radius (r_c= 2 nm) is presented in Fig. 4. a). Hole has higher wave function at the center of the dot and does not extend out of the dot. Maximum of hole radial probability is inside the dot, Fig. 3.a) and Fig 4. a). Electron wave function at the surface imply that electron behavior is more sensitive to changes at the surface. Electron and hole wave function overlap is high, implying short radiative lifetimes. Wave functions overlap slightly increases as the dimension of CdTe QD increases.

When ZnTe shell is added energetic scheme became as presented in Fig. 1. Transition energy E_{10} decreases as the ZnTe shell thickness increases, Fig. 2. This decrease is more significant for small QD core radius (r_c= 1 nm and r_c= 1.25 nm). Decrease is clearly visible in energetic scale in Fig. 2. For bigger QD core radius (r_c= 2.25 nm and r_c= 2.5 nm) this decrease is an order of magnitude lower.

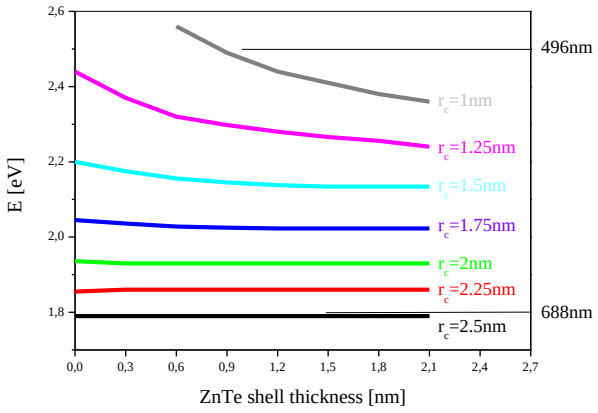

Fig. 2. Transition energy dependence on ZnTe shell thickness for different CdTe core radii.

When ZdTe shell is added to the small CdTe core, dimension of the whole dot changes drastically. Lowest electron and hole energies (E_{10}^e and E_{10}^h) of bare CdTe, before adding the shell, were higher than ZnTe barriers. Electron and hole tunnel easily through ZnTe shell, Fig. 3. b). The increased delocalization lowers confinement energy. When electron or hole energy in core/shell system become smaller than the ZnTe barriers they become less sensitive to shell thickness increase. Electron wave function slightly spread into the surrounding medium while hole wave function does not extend out of the dot. Wave function overlap slightly increases as ZnTe shell thickness increases.

In bigger CdTe QD, electron or both electron and hole lowest energies, E_{10}^{e} and E_{10}^{h}, are smaller than the ZnTe barriers. When ZnTe shell is added, dimension of the whole QD does not change dramatically, their energies stay almost unchanged. Like in small core radius QDs, holes does not extent to surrounding medium, electron extent but less than in small core radius case, Fig. 4. b).

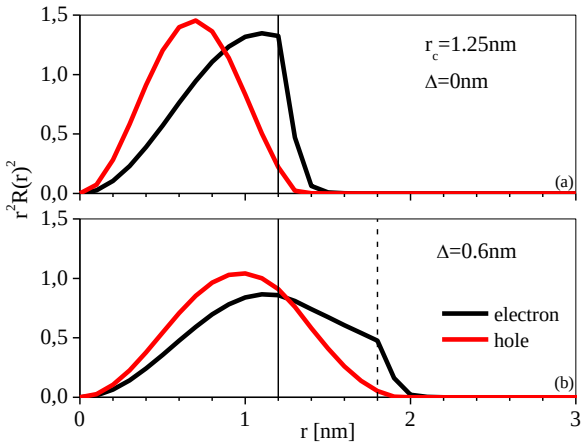

Fig. 3. Radial probability for a constant 1.25 nm radius core without shell a) and shell thickness Δ= 0.6 nm b).

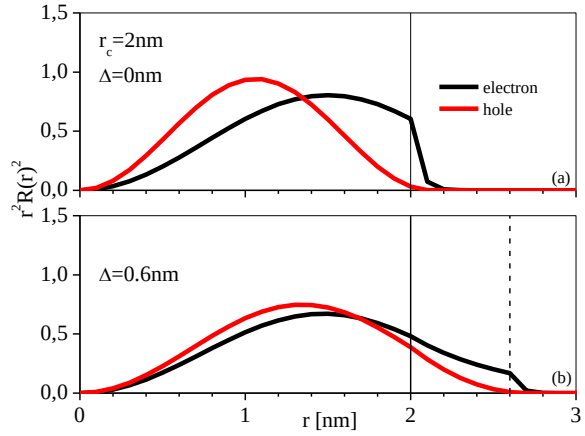

Fig. 4. Radial probability for a constant 2 nm radius core without shell a) and shell thickness Δ= 0.6 nm b).

In [10] authors present the quantum yield (QY) variation versus the Zn:Te precursor molar ratio and emission peak wavelength for CdTe/ZnTe QD samples synthesized in a one-pot-method. A narrow size distribution of core/shell particles was produced. From the plot, it is obvious that the QDs posses higher QY in red emission region. Red emission is large core radius dots characteristic. Authors emphasized that the size distribution is narrow. We assumed that the ratio of ZnTe shell volume to CdTe core volume in CdTe/ZnTe core/shell QDs is proportional to Zn:Cd precursor molar ratio. Transition energy E_{10} variation versus core radius and shell thickness is established from our calculations. If almost all Zn and Cd from precursor are in shell and core of QD, volume of ZnTe shell and volume of CdTe core reflect Zn:Cd precursor ratio. We used polynomial fit of experimental data, little bit different than in [10], to connect QY to Zn:Cd molar ratio and emission peak wavelength. We established relation between QY and the core/shell structure i.e. core radius and shell thickness. We present results for some core dimensions, Fig. 5.

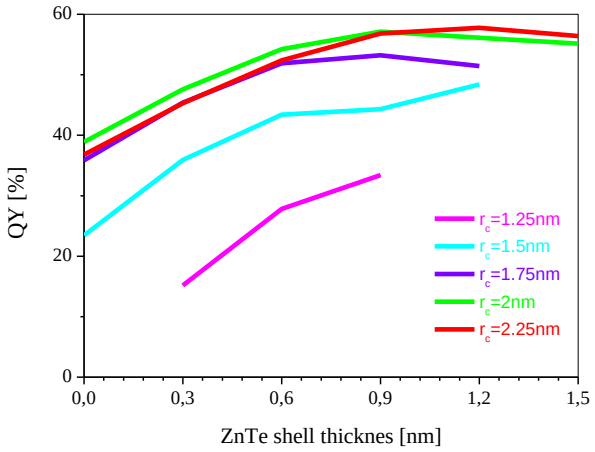

Fig. 5. QY dependence on ZnTe shell thickness for different CdTe core radii.

QY increases with shell thickness increase for all core radii. QY increases up to 0.6 nm ZnTe shell thickness. As we mentioned earlier, electron and hole wave overlap is high for all structures and slightly increases as the ZnTe shell dimension increases. This minor change in electron and hole wave overlap has negliable impact to QY increase. QY enhancement is a sign of successful surface vacancies and nonradiative recombination sites passivation. Defects in ZnTe shell may be the source of new nonradiative recombination sites in the shell that slow down QY increase for ZnTe shell wider than 0.6 nm.

3. Conclusion

In the bare CdTe dots the wave function of electron spreads over the entire particle and tunnel out into the surrounding medium while the heavier hole has higher probability in the center of the dot and does not extend into the surrounding medium. ZnTe shell prevent electrons to tunnel in surrounding medium. Effects of surface passivation result in QY increase. QY increases rapidly till 0.6 nm ZnTe shell thickness for all core radii. Despite the fact that offsets are not so high, especially for the hole, ZnTe protective shell in CdTe/ZnTe core/shell nanosystem is very efficient. ZnTe shell enhances QY, reduces toxicity and also improves their stability in biological environment.

Acknowledgments

This work was supported by Serbian Ministry of Education and Science (Projects No. III 45003 and III 45018).

References

[1] U. Woggon, Optical properties of Semiconductor Quantum Dots, Springer, Berlin (1997).
[2] W. C. W. Chan, S. M. Nie, Science **281**, 2016 (1988).
[3] M. Bruches, M. Moronne, P. Gin, S. Weiss, A. P. Alivisatos, Science **281**, 2013 (1988).
[4] C. Seydel, Science, **300**, 80 (2003).
[5] Chao Wang, Xue Gao, Xingguang Su, Anal Bioanal Chem **397**, 1397 (2010).
[6] F. Wang, W.B. Tan, Y. Zhang, X. P. Fan, M. Q. Wang, Nanotechnology **17**, R1-R13 (2006).
[7] L. F. Shi, V. De Paoli, N. Rozenzweig, Z. Rozenzweig, J. Am. Chem. Soc. **128**, 10378 (2006).
[8] S. J. Cho, D. Maysinger, M. Jain, B. Rder, S. Hackbarth, F. M. Winnik, Langmuir **23**(4), 1974 (2007).
[9] J. Ma, J. Chen, Y. Zhang, P. Wang, J. Guo, W. Yang, C. Wang, J. Phys. Chem. B **111**, 12012 (2007).
[10] W. Law, K. Yong, I. Roy, H. Ding, R. Hu, W. Zhao, P. Prasad, Small **5**(11), 1302 (2009.
[11] D. Schooss, A. Mews, A. Eychmuller, H. Weller, Phys. Rev. B **49**, 17072 (1994).
[12] N. V. Tkach, V. A. Golovatskii, O. M. Voitsekhivskaya, M. Ya. Mikhal'ova, R. B. Fartustinskii, Physics of the Solid State **43**, 1315 (2001).
[13] N. V. Tkach, Yu. A. Sety, Semiconductors **40**, 1083 (2006).
[14] T. Fromherz, F. Hauzenberger, W. Faschimger, M. Helm, P. Juza, H. Sitter, G. Bauer, Phys. Rev. B **47**, 1998 (1993).
[15] V. S. Bagaev, L. K. Vodop'yanov, V. S. Vinogradov, V. V. Zaitsev, S. P. Kozyrev, N. N. Mel'nik, E. E. Onishchenko, G. Karczewski, Physics of the Solid State **46**, 171 (2004).

*Corresponding author: dusanka@ipb.ac.rs